

ORIGINAL ARTICLE

# Application of Hybrid Matrix Metalloproteinase-Targeted and Dynamic <sup>201</sup>Tl Single-Photon Emission Computed Tomography/Computed Tomography Imaging for Evaluation of Early Post-Myocardial Infarction Remodeling

See Editorial by Schelbert

**BACKGROUND:** The induction of matrix metalloproteinases (MMPs) and reduction in tissue inhibitors of MMPs (TIMPs) plays a role in ischemia/reperfusion (I/R) injury post-myocardial infarction (MI) and subsequent left ventricular remodeling. We developed a hybrid dual isotope single-photon emission computed tomography/computed tomography approach for noninvasive evaluation of regional myocardial MMP activation with <sup>99m</sup>Tc-RP805 and dynamic <sup>201</sup>Tl for determination of myocardial blood flow, to quantify the effects of intracoronary delivery of recombinant TIMP-3 (rTIMP-3) on I/R injury.

**METHODS:** Studies were performed in control pigs (n=5) and pigs following 90-minute balloon occlusion-induced ischemia/reperfusion (I/R) of left anterior descending artery (n=9). Before reperfusion, pigs with I/R were randomly assigned to intracoronary infusion of rTIMP-3 (1.0 mg/kg; n=5) or saline (n=4). Three days post-I/R, dual isotope imaging was performed with <sup>99m</sup>Tc-RP805 and <sup>201</sup>Tl along with contrast cineCT to assess left ventricular function.

**RESULTS:** The ischemic to nonischemic ratio of <sup>99m</sup>Tc-RP805 was significantly increased following I/R in saline group (4.03±1.40), and this ratio was significantly reduced with rTIMP-3 treatment (2.22±0.57; P=0.03). This reduction in MMP activity in the MI-rTIMP-3 treatment group was associated with an improvement in relative MI region myocardial blood flow compared with the MI-saline group and improved myocardial strain in the MI region.

**CONCLUSIONS:** We have established a novel hybrid single-photon emission computed tomography/computed tomography imaging approach for the quantitative assessment of regional MMP activation, myocardial blood flow, and cardiac function post-I/R that can be used to evaluate therapeutic interventions such as intracoronary delivery of rTIMP-3 for reduction of I/R injury in the early phases of post-MI remodeling.

Stephanie L. Thorn, PhD  
Shayne C. Barlow, DVM, PhD, DACLAM  
Attila Feher, PhD, MD  
Mitchel R. Stacy, PhD  
Heather Doviak, MSc  
Julia Jacobs, BSc  
Kia Zellars, MSc  
Jennifer M. Renaud, MSc  
Ran Klein, PhD  
Robert A. deKemp, PhD  
Aarif Y. Khakoo, MD  
TaeWeon Lee, PhD  
Francis G. Spinale, PhD, MD  
Albert J. Sinusas, MD

**Key Words:** balloon occlusion  
■ matrix metalloproteinases  
■ myocardial infarction  
■ reperfusion injury  
■ ventricular remodeling

© 2019 American Heart Association, Inc.

<https://www.ahajournals.org/journal/circimaging>

## CLINICAL PERSPECTIVE

Myocardial infarction (MI) is prevalent occurring in >1.2 million patients annually. Following ischemia-reperfusion post-MI, there is activation of proteolytic enzymes, matrix metalloproteinases that degrade the extracellular matrix within the MI region. This process results in structural alterations, infarct expansion, and adverse remodeling that can result in heart failure. In the current study, we developed and applied an advanced noninvasive dual isotope hybrid single-photon emission computed tomography/computed tomography imaging approach that provides a regional map of matrix metalloproteinase activation in the myocardium in conjunction with quantification of regional myocardial blood flow and function. This approach can be performed early following ischemia-reperfusion injury and can be used to guide and evaluate novel therapies to prevent post-MI remodeling. This methodology was specifically used to assess therapeutic intracoronary delivery of a matrix metalloproteinase inhibitor, recombinant tissue inhibitors of matrix metalloproteinases-3, to the MI region, demonstrating a reduction in matrix metalloproteinase activity as measured by single-photon emission computed tomography imaging of a matrix metalloproteinase-targeted imaging agent,  $^{99m}\text{Tc}$ -RP805, an increase in myocardial blood flow with dynamic  $^{201}\text{Tl}$  imaging, and an improvement in left ventricular strain on cine computed tomography. This novel hybrid imaging approach confirmed the therapeutic benefit of the intracoronary delivery of recombinant tissue inhibitors of matrix metalloproteinases-3 early following ischemia-reperfusion injury.

The emphasis on early reperfusion strategies following acute myocardial infarction (MI) has resulted in complicating left ventricular (LV) myocardial injury due to ischemia-reperfusion (I/R). While several biological pathways are evoked early in the post I/R period, both basic and clinical studies have uniformly identified that an induction in the family of proteases, the matrix metalloproteinases (MMPs), occurs.<sup>1</sup> While the substrates for these MMPs were canonically thought to be extracellular matrix proteins such as collagens, it is now recognized that the substrate portfolio is diverse and includes processing of a number of biological signaling molecules.<sup>2</sup> In clinical observational studies, plasma levels of MMPs increase significantly and have been related to the degree of adverse LV remodeling in the early I/R period.<sup>3</sup> In animal studies, a cause-effect relationship between MMP induction, LV injury and remodeling in the context of

ischemia has been established.<sup>4-7</sup> However, these studies were hampered by the fact that quantification of MMP activity was through indirect measurement of circulating biomarkers or in vitro surrogate methods and that actual LV myocardial MMP activity was not directly assessed. Past studies from this laboratory have established a novel strategy by which MMP activity can be visualized within the myocardium utilizing a single-photon emission computed tomography (SPECT) imaging approach using a  $^{99m}\text{Tc}$ -labeled MMP targeted radiotracer ( $^{99m}\text{Tc}$ -RP805).<sup>8-10</sup> While our previous studies have validated this MMP activity imaging approach with permanent coronary occlusion, it remains unknown whether and to what degree these prior findings can be extended to a clinically relevant context of I/R injury, as well as at an early time point post reperfusion ( $\approx 72$  hours post-I/R). We propose to apply a novel hybrid SPECT/CT dual isotope imaging approach that incorporates  $^{99m}\text{Tc}$ -RP805 for in vivo evaluation of regional myocardial MMP activity, with dynamic  $^{201}\text{Tl}$  imaging for quantitative evaluation of regional myocardial blood flow (MBF), and contrast cine CT imaging to evaluate changes in regional myocardial strain, and global function in the early post-I/R period. Accordingly, the first objective of this study was to demonstrate that targeted MMP imaging can be successfully performed in the early post I/R period using a clinically relevant large animal (pig) model and to also examine regional MBF and function, using a multi-modality imaging approach.

MMP activity is tightly controlled at several levels including both transcriptional and post-translational regulation.<sup>2</sup> With respect to post-transcriptional regulation, the endogenous tissue inhibitors of the MMPs (TIMPs) have been shown to play an important role in the context of LV remodeling.<sup>11</sup> For example, transgenic deletion of a specific TIMP, TIMP-3, was shown to exacerbate LV remodeling and dysfunction following an ischemic insult.<sup>12</sup> In clinical observational studies, the relative magnitude of plasma TIMP-3 levels in the early post-I/R period is significantly blunted when compared with MMP release.<sup>13-15</sup> In more recent studies, myocardial supplementation (by direct injection or by intracoronary delivery) of recombinant TIMP-3 (rTIMP-3) has been shown to mitigate adverse LV remodeling in the early postischemic period.<sup>16-19</sup> However, direct in vivo assessment of MMP activity following rTIMP-3 delivery in the context of I/R has not been performed. Accordingly, the second objective of this study was to examine regional LV MMP activity following intracoronary delivery of rTIMP-3 in the context of the early post-I/R period. Moreover, this targeted MMP imaging approach was integrated with assessment of regional MBF and function.

## METHODS

The experimental and imaging approach are provided herein (Figure 1), with expanded methodological detail provided in the [Data Supplement](#). The authors declare that all supporting data are available within the article ([Data Supplement](#)).

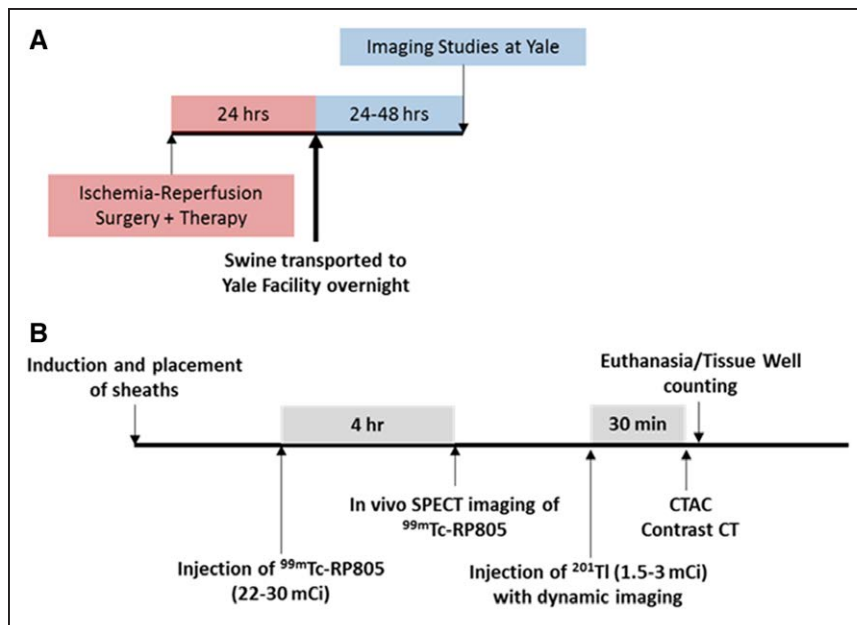


**Figure 1. Experimental Protocols.**

Experimental timelines for the ischemia-reperfusion surgery to acute imaging studies at Yale (A) and the imaging studies at the Yale facility (B). CT indicates computed tomography; and SPECT, single-photon emission computed tomography.

## rTIMP-3 Formulations

The rTIMP-3 formulation and intracoronary dose used was previously evaluated for efficacy in prior intracoronary delivery studies.<sup>16</sup>

## I/R Induction and rTIMP-3 Delivery

This multi-institutional study was approved by the institutional animal care and use committees at both the University of South Carolina School of Medicine and Yale University School of Medicine and according to the National Institutes of Health Guidelines for Care and Use of Laboratory Animals. Mature Yorkshire male pigs (n=9; 25–30 kg) were anesthetized (1.5%–2% isoflurane; [Data Supplement](#)), and under fluoroscopic guidance (GE OEC 9600, UT), the left anterior descending artery below the first diagonal branch underwent balloon occlusion for 90 minutes. At the final 4 minutes of the occlusion period, the pigs were randomized to receive either intracoronary rTIMP-3 (1.0 mg/kg, MI-rTIMP3 group, n=5) or saline (MI-saline group, n=4) contained in a total 1 mL volume.<sup>16</sup> One day following I/R induction, the pigs were transported to the Yale Translational Research Imaging Center for the imaging studies (Figure 1A). A separate cohort of control pigs that had no coronary intervention underwent imaging and were analyzed in identical fashion to establish referent normal values.

## In Vivo Dual-Isotope Hybrid SPECT/CT Imaging

The pigs were anesthetized (1.5%–2% isoflurane), and central access catheters placed for intravenous injection of  $^{99m}\text{Tc}$ -RP805 (22–32 mCi), an in vivo marker of MMP activation. This MMP-targeted radiotracer binds to the catalytic domain of all major MMP types, but not to other proteolytic enzymes.<sup>8,20</sup> Approximately 4 hours following the  $^{99m}\text{Tc}$ -RP805 injection, an initial 15-minute SPECT/CT image was acquired followed by injection of  $^{201}\text{Tl}$  (1.5–3 mCi) and dual

isotope dynamic SPECT/CT image was acquired over 30 minutes.

## Dual Isotope SPECT/CT Imaging Methods

SPECT/CT images were acquired on a hybrid dedicated cardiac cadmium-zinc-telluride SPECT/64-slice CT imaging system (Discovery 570c NM/CT, GE Healthcare; see Figure 1B for overview of imaging protocol). Two consecutive 15-minute list-mode scans were acquired followed by a noncontrast CT ([Data Supplement](#)). SPECT images were reconstructed using standardized iterative algorithms previously validated.<sup>21</sup> An ECG-gated contrast CT was then acquired and endocardial and epicardial LV surfaces identified and used to compute volumes, left-ventricular ejection fraction (LVEF), and regional peak circumferential and radial strain as detailed in the [Data Supplement](#). The mid-anteroseptal region was analyzed as representative of the central MI region and compared with the contralateral remote mid-lateral wall (Figure 1 in the [Data Supplement](#)).

## Ex vivo SPECT/CT Imaging and Tissue Gamma Well Counting

After completion of in vivo imaging, the pigs were euthanized, and hearts excised. The excised hearts were then cast and placed back in the hybrid SPECT/CT imaging system for high resolution ex vivo imaging for optimal evaluation of the 3-dimensional distribution of radiotracer activity ([Data Supplement](#)). The LV was sliced into 4-mm thick short axis slices from base to apex, and each slice was digitally photographed for analysis of MI size. Each slice was then divided into 8 radial pies and further divided into epicardial and endocardial pieces for gamma well counting for quantitative determination of regional myocardial activity ([Data Supplement](#)). The absolute uptake of each tracer was computed as the percent injected dose per gram of tissue (%ID/g), with values displayed as a circumferential profile, as illustrated in Figure 2. Tissue segments with values >70% of the overall maximum  $^{201}\text{Tl}$  LV uptake were categorized as normal regions and segments with <70% of the maximum  $^{201}\text{Tl}$  uptake were considered the MI region.

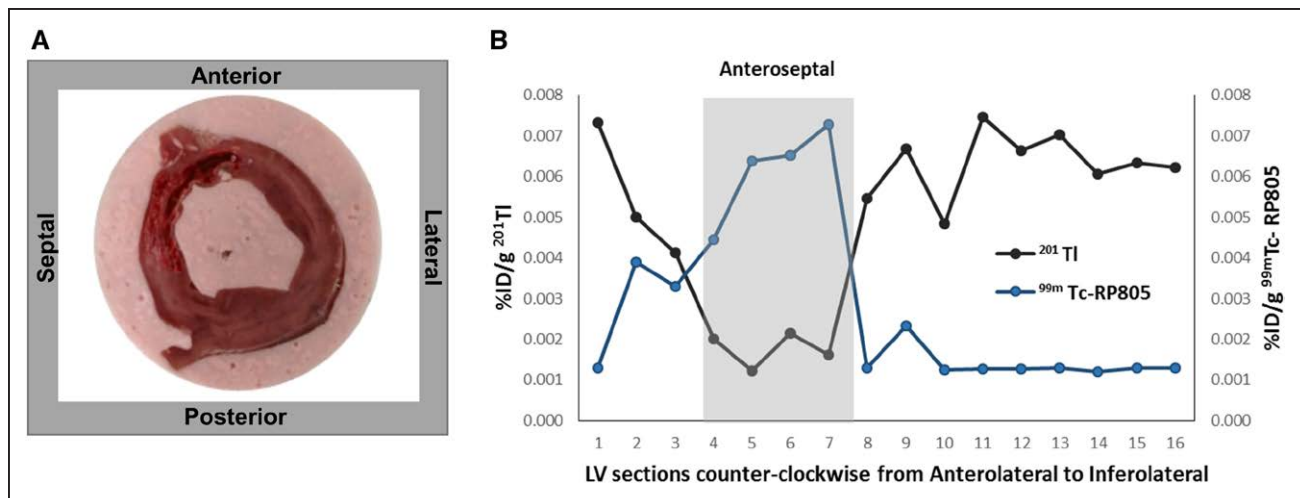


**Figure 2.** Postmortem analysis of myocardial radiotracer uptake.

A representative short-axis postmortem slice is shown with an anteroseptal infarct (A). Hearts were cut in 4-mm thick slices and cut into 8 radial pies, subdivided into endocardial and epicardial segments. Myocardial radioactivity was assessed by gamma well counting, expressed as absolute uptake (%ID/g), and results displayed as circumferential profiles from the anterolateral to inferolateral wall in a counter-clockwise direction (B). <sup>99m</sup>TcRP805 uptake (blue) was increased in the myocardial infarction area (gray shaded area) that demonstrated decreased <sup>201</sup>Tl uptake (black). LV indicates left ventricular.

### Statistical Analyses

All data are expressed as mean±SD of the mean. The comparative analysis between the means of the controls, MI-saline, and MI-rTIMP3-treated animals was assessed with a 1-way ANOVA using post hoc Bonferroni analysis performed with SPSS software (version 24.0, SPSS, Inc). The comparison of means for MBF was assessed with a 2-way ANOVA with a Sidak multiple comparison test and comparison of <sup>99m</sup>Tc-RP805 uptake ratio assessed with an unpaired *t* test performed in GraphPad Prism. A *P*<0.05 was considered significant.

## RESULTS

### Global and Regional LV Function Early Post-I/R

At 3 to 4 days post-I/R, both MI treatment groups demonstrated a significant reduction in LVEF compared with the control group (Table). Although there was an improvement in LVEF in the MI-rTIMP3 group, this did not achieve statistical significance (*P*=0.36) at this early time point post I/R.

Examples of short-axis CT images with superimposed endocardial and epicardial contours are shown for representative pigs from each group (Figure 3A). Corresponding color-coded polar maps are shown below for peak circumferential strain (Figure 3B) and peak radial strain (Figure 3C). Peak circumferential strain was significantly (*P*=0.01) reduced in the MI region of the MI-saline group (Table; Figure 4A) compared with controls, although relatively preserved in the MI-rTIMP3 group. Peak radial strain was also significantly reduced in the MI region of the MI-saline group compared with controls (*P*<0.02; Table), and again relatively preserved in the MI-rTIMP3 group. We also observed an increase in radial strain in the remote area of the MI-saline group (*P*=0.05; Table) compared with controls, which was not seen in the MI-rTIMP3 group (Figure 4B).

### Quantitative Myocardial <sup>201</sup>Tl Flow

The mid-wall anteroseptal region was analyzed and served as representative of the central reperfused MI region and compared with the normal contralateral remote mid-wall lateral region (Figure I in the Data Supplement).

**Table.** Global and Regional LV Function

	Controls (n=4)	MI Only (n=4)	<i>P</i> Value	rTIMP-3 1.0 mg/kg (n=5)	<i>P</i> Value
LVED volume, mL	72.8±21.1	57.3±16.5	1.00	67.5±30.5	1.00
LVES volume, mL	35.5±17.9	43.2±15.0	1.00	48.9±25.7	1.00
LVEF (%)	53.2±14.2	25.3±6.4	0.01	30.1±8.0	0.02
Peak circumferential strain (remote area)	-10.3±1.69	-10.71±1.45	1.00	-7.76±3.38	0.48
Peak circumferential strain (infarct area)	-13.40±3.05	-1.47±2.58	0.01	-7.34±4.34	0.08
Peak radial strain (remote area)	20.18±6.47	32.52±5.49	0.05	26.02±6.19	0.55
Peak radial strain (infarct area)	19.94±6.62	1.33±4.13	0.02	9.56±9.45	0.19

LVED indicates left ventricular end-diastolic; LVEF, left ventricular ejection fraction; LVES, left ventricular end-systolic; MI, myocardial infarction; and rTIMP-3, recombinant tissue inhibitors of matrix metalloproteinases-3.

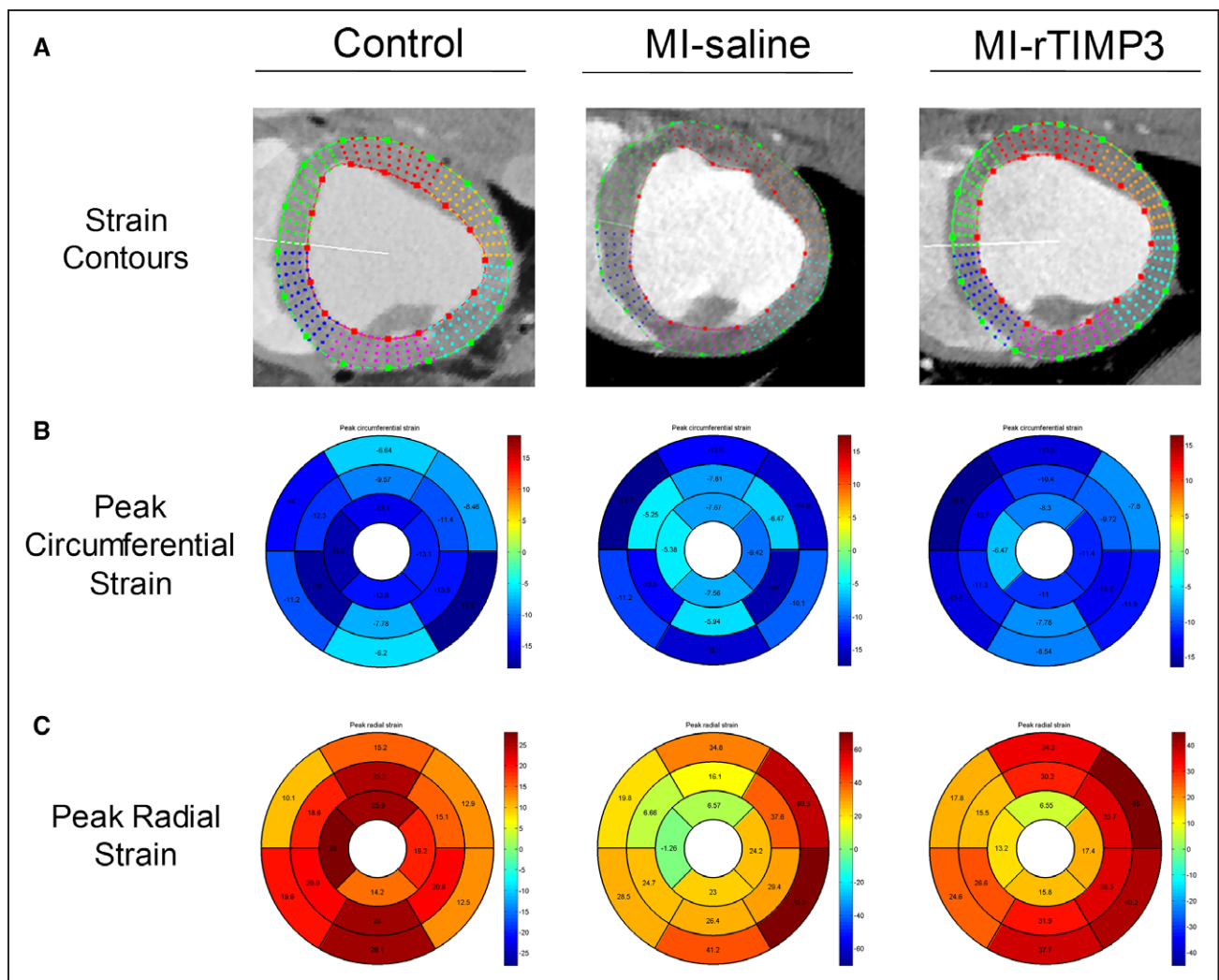


**Figure 3. Contrast computed tomography (CT) images and strains.**

Representative contrast CT images are shown from a control, myocardial infarction (MI)-saline and an MI-recombinantTIMP3 (rTIMP3) pig with the corresponding endocardial (red) and epicardial (green) contours (A). These contours were used to compute regional peak circumferential left ventricular strain (B) and peak radial strain (C) for each of the 17 American Heart Association segments, excluding apex. Color scale bars are associated with each map. TIMP indicates tissue inhibitors of matrix metalloproteinases.

Representative quantitative polar maps of regional quantitative myocardial flow (K1) derived from dynamic <sup>201</sup>Tl SPECT imaging with kinetic modeling are shown for representative pigs from each group (Figure 5A). There were no significant regional differences in myocardial flow in control pigs. The MI-saline pigs demonstrated a significant ( $P=0.018$ ) reduction in <sup>201</sup>Tl MBF in the MI region relative to control remote regions of the heart (Figure 5B). However, MBF in the MI region of the MI-r-TIMP3 group was similar to remote region ( $P=0.80$ ), suggesting a relative preservation of MBF in the MI region following intracoronary infusion of rTIMP-3.

### Dual Isotope <sup>99m</sup>Tc-RP805 and <sup>201</sup>Tl SPECT Imaging

In vivo dual isotope <sup>99m</sup>Tc-RP805 and <sup>201</sup>Tl SPECT/CT imaging demonstrated increased focal uptake of <sup>99m</sup>Tc-RP805 within the MI region that corresponded with the <sup>201</sup>Tl per-

fusion defect. Representative hybrid SPECT/CT images are shown for a pig in the MI-saline group (Figure 6). This pattern of mismatch between MMP activation and perfusion was consistently observed in the MI-saline group. Qualitatively, the MI-rTIMP3 group demonstrated a less dramatic increase in <sup>99m</sup>Tc-RP805 uptake within the MI region on the delayed static <sup>99m</sup>Tc-RP805 in vivo SPECT images.

Ex vivo SPECT/CT imaging was used to evaluate relative myocardial <sup>201</sup>Tl perfusion and <sup>99m</sup>Tc-RP805 uptake in MI-saline and MI-rTIMP3 groups to avoid any confounding effects of motion or extracardiac activity. Representative bullseye maps of <sup>201</sup>Tl perfusion and <sup>99m</sup>Tc-RP805 uptake are shown in Figure 7A.

### Myocardial Gamma Well Counting of <sup>99m</sup>Tc-RP805 and <sup>201</sup>Tl

The results from gamma well counting of myocardial tissue are shown in Figure 7B. Myocardial segments were

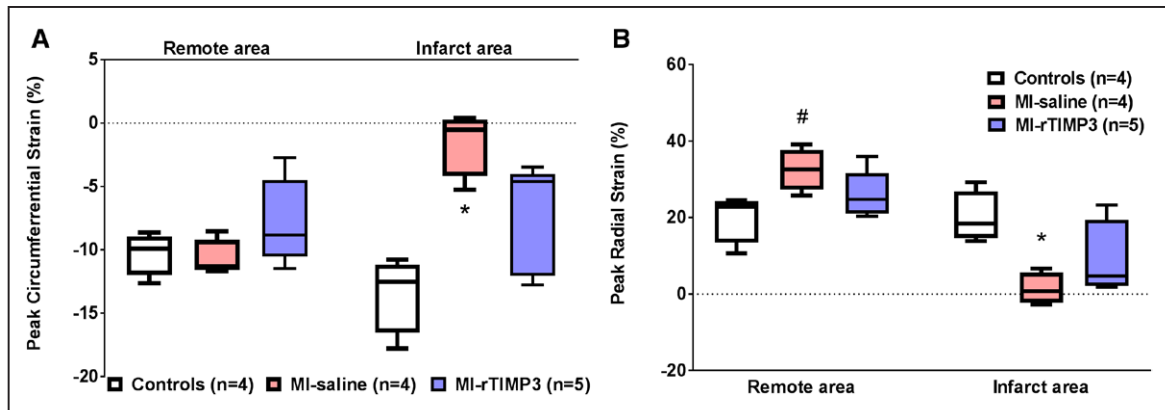


**Figure 4. Alterations in myocardial strain.**

Box plots of average peak left ventricular (LV) circumferential strain (A) and peak LV radial strain (B) illustrating the full range of data. There was a significant decrease in both the peak circumferential ( $P=0.01$ ) and radial strain ( $P=0.02$ ) in the myocardial infarction (MI) area for the MI-saline group compared with non-MI controls. Additionally, there was an increase in peak radial strain in the remote zone of the MI-saline group vs controls ( $P=0.05$ ). This compensatory increase in remote radial strain was not seen in the MI-recombinant TIMP-3 (rTIMP3) group. \* $P<0.05$  vs non-MI controls, # $P=0.05$ , 1-way ANOVA, with Bonferroni post hoc correction. TIMP indicates tissue inhibitors of matrix metalloproteinases.

separated into MI and remote non-MI regions based on relative  $^{201}\text{Tl}$  activity. There was an increase in relative  $^{99\text{m}}\text{Tc}$ -RP805 uptake in the MI region in both MI groups (MI-saline:  $4.03\pm 1.40$ ; MI-rTIMP3:  $2.22\pm 0.57$ ). However, the increase  $^{99\text{m}}\text{Tc}$ -RP805 uptake in the MI-rTIMP3 group was approximately half that seen in MI-saline group (Figure 7B).

### Ex Vivo Infarct size

Postmortem analyses demonstrated a slight but non-significant decrease in MI size in the MI-rTIMP3 group versus the MI-saline group when expressed as a percentage of total LV area at this early time point post-MI (MI-rTIMP3:  $14\pm 9\%$ ; MI-saline:  $21\pm 5\%$ ,  $P=0.21$ ).

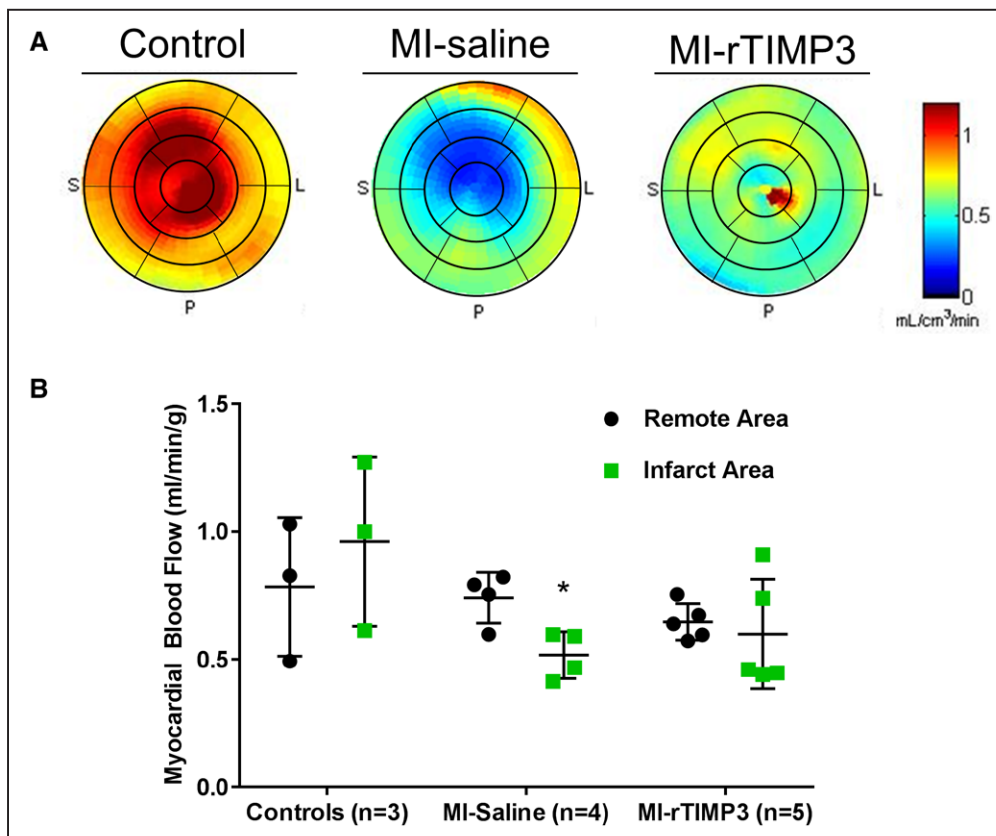


**Figure 5. Quantitative regional myocardial blood flow determined from in vivo dynamic  $^{201}\text{Tl}$ -single-photon emission computed tomography imaging and kinetic modeling.**

Shown are representative myocardial flow (K1) polar maps for each group (A). There is a significant reduction in perfusion in the infarct territory compared with the contralateral remote area in the myocardial infarction (MI)-saline group ( $P=0.02$ ), although there was no significant reduction in myocardial blood flow in the MI-recombinant TIMP-3 (rTIMP3) group ( $P=0.80$ ; B). \* $P<0.05$  vs remote, 2-way ANOVA. TIMP indicates tissue inhibitors of matrix metalloproteinases.

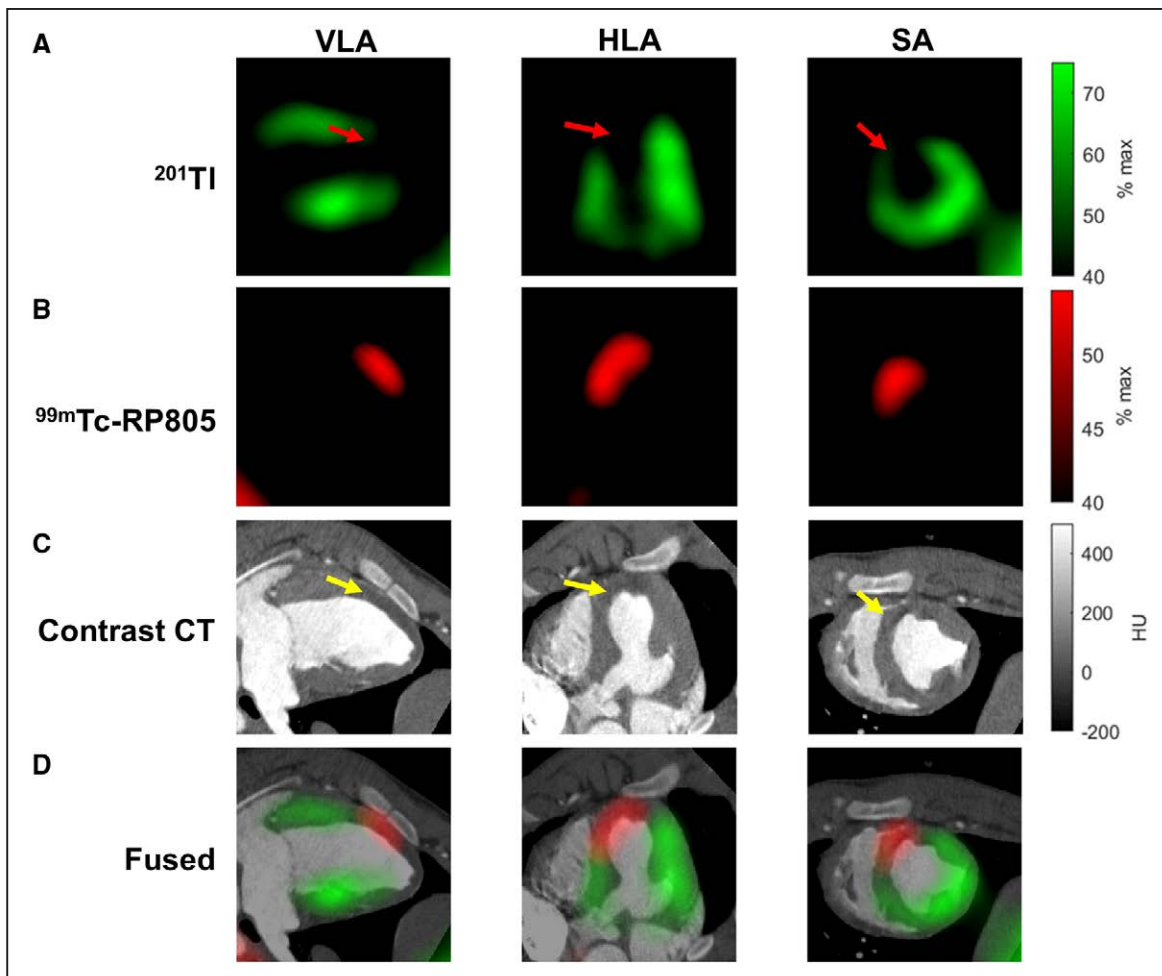


**Figure 6.** Representative in vivo hybrid dual isotope single-photon emission computed tomography (SPECT)/CT images are shown in vertical long axis (VLA), horizontal long axis (HLA), and short axis (SA) from a myocardial infarction-Saline pig.

$^{201}\text{Tl}$  SPECT images are shown in green (A),  $^{99\text{m}}\text{Tc}$ -RP805 uptake in red (B), and contrast CT in black and white (C). A dense  $^{201}\text{Tl}$  perfusion defect (red arrow) is seen in the anteroseptal wall with corresponding hypoperfusion zone on the contrast CT image (yellow arrow). The fusion of the SPECT and CT images (D) demonstrates focal  $^{99\text{m}}\text{Tc}$ -RP805 uptake within the perfusion defect.

## DISCUSSION

The current study demonstrates that dual isotope  $^{99\text{m}}\text{Tc}$ -RP805 and  $^{201}\text{Tl}$  hybrid SPECT/CT imaging can quantify myocardial MMP activation and regional MBF in a large animal model of I/R injury with contrast cineCT for assessment of regional myocardial strain. This is the first study to demonstrate that regional MMP activity changes as a function of intracoronary delivery of a recombinant pharmacological agent, in this case, intracoronary delivery of rTIMP-3. The reduction in MMP activation in the MI region was associated with both an improvement in quantitative MBF and a preservation of regional circumferential and radial strain in the early period following I/R. This multimodality imaging approach offers a noninvasive method to potentially guide and evaluate novel early therapeutic intervention to reduce reperfusion injury and modulate late post-MI remodeling and long term outcome.

## Model of Reperfusion Injury

MI remains one of the leading causes of morbidity and mortality, and the primary focus has been to reduce MI size by limiting damage during ischemia such as the prevention of the reperfusion injury.<sup>22–25</sup> The current study used a porcine model of I/R injury to recapitulate the reperfusion injury that can be encountered following percutaneous coronary interventions with acute coronary syndromes. Specifically, a period of 90 minutes of coronary occlusion followed by reperfusion is not dissimilar to clinical context of door-to-balloon times of <90 minutes.<sup>26–28</sup> This model also allows use of standard clinical imaging systems which facilitates translation of these imaging approaches. This large animal model also reproduces the fundamental characteristics of the process of repair and myocardial remodeling, alterations in regional and global perfusion, and changes in wall thickness and function.<sup>29</sup>

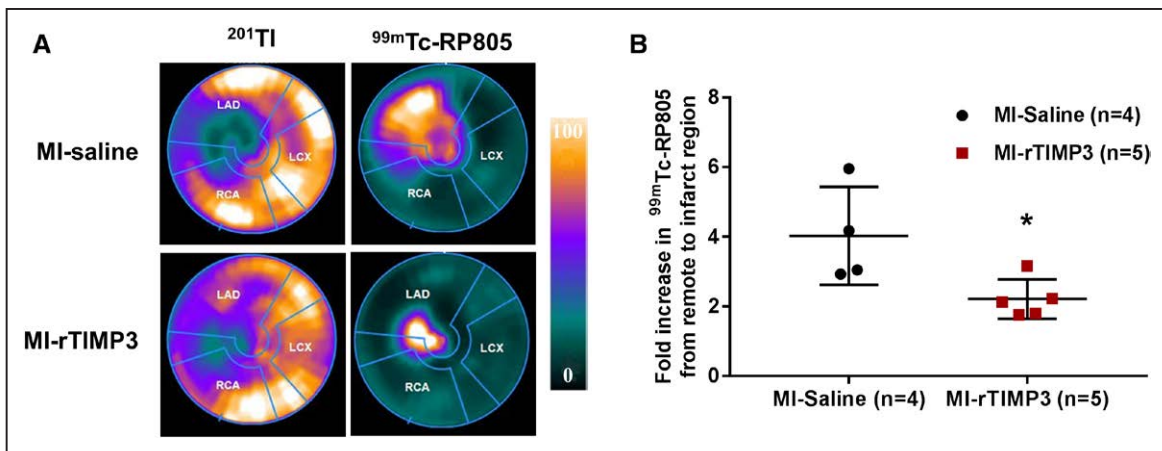


**Figure 7.** Effects on  $^{201}\text{Tl}$  and  $^{99m}\text{Tc-RP805}$  myocardial uptake.

Representative ex vivo single-photon emission computed tomography (SPECT) left ventricular polar maps of relative  $^{201}\text{Tl}$  and  $^{99m}\text{Tc-RP805}$  uptake from both myocardial infarction (MI) groups (A). Well counting of myocardial tissue demonstrated an increase in  $^{99m}\text{Tc-RP805}$  uptake in the MI region (B). However, there was a significant reduction in relative myocardial  $^{99m}\text{Tc-RP805}$  uptake in MI region relative to control region in the MI-recombinant TIMP-3 (rTIMP3) group compared with MI-saline group ( $P=0.03$ ). \* $P=0.03$  vs MI-saline group, Student *t* test. TIMP indicates tissue inhibitors of matrix metalloproteinases.

### Dynamic SPECT/CT Imaging

The hybrid SPECT/CT approach has been previously used quite successfully for the purposes of measuring serial changes in myocardial perfusion in swine.<sup>21</sup> In the current study, we utilized dynamic hybrid  $^{201}\text{Tl}$  SPECT imaging for quantification of MBF. This dynamic imaging was facilitated by a high-resolution high-sensitivity SPECT/CT camera with  $180^\circ$  of cadmium-zinc-telluride detectors that can simultaneously acquire 3-dimensional data with improved resolution compared with a more conventional dual-headed SPECT camera with sodium-iodide (NaI) detectors. The high sensitivity of this imaging system allows for dynamic imaging and quantification of MBF at relatively low doses of radiation (<6–10 mSv). The improved energy resolution of cadmium-zinc-telluride over conventional NaI detectors permitted dual isotope physiological imaging with  $^{201}\text{Tl}$  in conjunction with the targeted  $^{99m}\text{Tc}$ -labeled molecular radiotracer.

While improvement in LV global function with measurement of LVEF is commonly used to assess functional changes associated with post-MI remodeling, recent studies have indicated that strain assessed with echocardiography can have predictive value on myocardial functional recovery.<sup>30</sup> We demonstrated that high-resolution cine CT performed with a low dose of a standard iodinated contrast agent can also provide precise LV regional myocardial circumferential and radial strain measurements. Circumferential strain has been recently reported to have a prognostic importance in patient's post-MI.<sup>31</sup> These authors propose that circumferential strain may be more indicative over longitudinal strain of myocardial salvage and the propensity to recover LV function in the longer term.<sup>31</sup> Indeed, this identical swine IR model and rTIMP-3 intracoronary therapy resulted in an improvement in LVEF at 4 weeks post-MI.<sup>16</sup>

### MMPs and TIMPs in Post-MI Remodeling and Dual Isotope Hybrid SPECT/CT Imaging

Previous basic and clinical studies have identified that the induction of MMPs, and reduction in endogenous TIMPs play a contributory role in early ischemic injury and late LV remodeling.<sup>10,12,14,32–37</sup> Circulating MMP plasma levels are elevated in patients following MI and seems to serve as a predictor for development of heart failure.<sup>15,35,38</sup> However, despite a large number of mechanistic studies implicating MMP activation and adverse LV remodeling, clinical trials employing systemic pharmacological MMP inhibition have yielded mixed results (Tetracycline [Doxycycline] and Post Myocardial Infarction Remodeling; Prevention of Myocardial Infarction Early Remodeling).<sup>39–41</sup> This may be due in part, to the lack of a direct approach to assess therapeutic targeting of MMP activation within the LV myocardium. Previous studies have investigated the use of targeted TIMP-3 delivery to the MI region and reported reduced adverse post-MI remodeling.<sup>14,17,18</sup> More recently, it was established that intracoronary delivery of rTIMP-3 in pigs at the time of reperfusion favorably reduced LV remodeling and indices of heart failure progression.<sup>16</sup> The present study critically advanced this field of pharmacological therapy by directly demonstrating that intracoronary rTIMP-3 delivery effectively reduced MMP activity in the targeted LV region following I/R. Our prior work demonstrated that  $^{99m}\text{Tc-RP805}$  uptake was increased within the MI region at 1 week post-MI induced by permanent coronary occlusion, and this increase was correlated to changes in the activity of several MMP types.<sup>10</sup> However, these prior MMP targeted imaging studies employed models of permanent coronary occlusion without reperfusion.<sup>9,10</sup> In the current study, using a model of I/R, intracoronary delivery

of rTIMP-3 improved regional MBF within the MI region, suggesting a potential reduction in the no reflow associated with reperfusion injury. Although we did not demonstrate a significant difference in LVEF at this early time point post-rTIMP-3 delivery, previous work demonstrate that intracoronary rTIMP-3 did result in an improvement of global LV function at 1-month post-MI.<sup>16</sup> However, the present study did demonstrate in this early I/R time period that rTIMP-3 improved regional myocardial strain within the MI region which in turn over time may contribute to improved LV pump function, as reported previously.<sup>16</sup>

## Limitations and Summary

The current study was limited to only the early evaluation of myocardial MMP activation with <sup>99m</sup>Tc-RP805 post-MI and the effects of intracoronary rTIMP-3 delivery. Based on these unique proof of concept studies, combined imaging/pharmacological studies are warranted. There does seem to be a partial volume effect in the apical region of the in vivo MBF imaging results; however, the apical segments were not included in the evaluation of MBF. We also did not specifically demonstrate that myocardial uptake of <sup>99m</sup>Tc-RP805 in the current study correlated with other molecular markers of MMP activation, although this has been done in previous studies.<sup>10,16</sup> Nevertheless, this study establishes the utility of a clinically relevant noninvasive imaging approach that can directly visualize and quantify regional myocardial MMP activation in relation to changes in critical physiological indices of regional MBF and function. The application of this dual isotope hybrid SPECT/CT imaging approach may facilitate the optimization and translation of therapeutic interventions post-MI such as the use of intracoronary delivery of recombinant peptides for reduction of I/R injury in the early stages of post-MI remodeling.

## ARTICLE INFORMATION

Received February 25, 2019; accepted August 28, 2019.

The Data Supplement is available at <https://www.ahajournals.org/doi/suppl/10.1161/CIRCIMAGING.119.009055>.

## Correspondence

Albert J. Sinusas, MD, Yale Translational Research Imaging Center, Yale University School of Medicine, Yale University, PO Box 208017, DANA-3, New Haven, CT, 06520. Email [albert.sinusas@yale.edu](mailto:albert.sinusas@yale.edu).

## Affiliations

Section of Cardiovascular Medicine, Department of Internal Medicine (S.L.T., A.F., M.R.S., A.J.S.) and Department of Radiology and Biomedical Imaging (A.J.S.), Yale University, School of Medicine, New Haven, CT. Yale Translational Research Imaging Center, Department of Internal Medicine, New Haven, CT (S.L.T., A.F., M.R.S., A.J.S.). Department of Cell Biology and Anatomy, Surgery, Cardiovascular Translational Research Center, WJB Dorn Veteran Affairs Medical Center, University of South Carolina School of Medicine, Columbia (S.C.B., H.D., J.J., K.Z., F.G.S.). Division of Cardiology, University of Ottawa Heart Institute, ON, Canada (J.M.R., R.K., R.d.K.). Amgen, CardioMetabolic Disorders, South San Francisco, CA (A.Y.K., T.W.).

## Acknowledgments

We acknowledge the assistance of the University of South Carolina and Yale University veterinarian staff in their assistance with ensuring the health and well-being of the animals in this study. We also acknowledge the technical assistance of Christi Hawley, Tsa Shelton, and Eva Romito.

## Sources of Funding

This work was supported by the NH grants HL098069 (Dr Sinusas), HL113352 (Dr Sinusas), S10RR025555 (Dr Sinusas), HL131280 (Dr Spinale), HL130972 (Dr Spinale), and basic research grant from Amgen Incorporated.

## Disclosures

Dr Spinale is the founder of MicroVide, LLC, and Dr Sinusas is a limited partner and consultant of MicroVide, LLC, which holds the license for the use of <sup>99m</sup>Tc-RP805 in myocardial applications. Drs Khakoo and Lee are employees of Amgen Incorporated, which provided the rTIMP-3 formulation under a material transfer agreement from Amgen to Dr Spinale. J.M. Renaud, Dr Klein, Dr deKemp receive revenue shares from the sales of FlowQuant software.

## REFERENCES

- Cheung PY, Sawicki G, Wozniak M, Wang W, Radomski MW, Schulz R. Matrix metalloproteinase-2 contributes to ischemia-reperfusion injury in the heart. *Circulation*. 2000;101:1833–1839. doi: 10.1161/01.cir.101.15.1833
- Spinale FG. Myocardial matrix remodeling and the matrix metalloproteinases: influence on cardiac form and function. *Physiol Rev*. 2007;87:1285–1342. doi: 10.1152/physrev.00012.2007
- Webb CS, Bonnema DD, Ahmed SH, Leonardi AH, McClure CD, Clark LL, Stroud RE, Corn WC, Finklea L, Zile MR, et al. Specific temporal profile of matrix metalloproteinase release occurs in patients after myocardial infarction: relation to left ventricular remodeling. *Circulation*. 2006;114:1020–1027. doi: 10.1161/CIRCULATIONAHA.105.600353
- Mukherjee R, Brinsa TA, Dowdy KB, Scott AA, Baskin JM, Deschamps AM, Lowry AS, Escobar GP, Lucas DG, Yarbrough WM, et al. Myocardial infarct expansion and matrix metalloproteinase inhibition. *Circulation*. 2003;107:618–625. doi: 10.1161/01.cir.0000046449.36178.00
- Lindsey M, Wedin K, Brown MD, Keller C, Evans AJ, Smolen J, Burns AR, Rossen RD, Michael L, Entman M. Matrix-dependent mechanism of neutrophil-mediated release and activation of matrix metalloproteinase 9 in myocardial ischemia/reperfusion. *Circulation*. 2001;103:2181–2187. doi: 10.1161/01.cir.103.17.2181
- Wang W, Schulze CJ, Suarez-Pinzon WL, Dyck JR, Sawicki G, Schulz R. Intracellular action of matrix metalloproteinase-2 accounts for acute myocardial ischemia and reperfusion injury. *Circulation*. 2002;106:1543–1549. doi: 10.1161/01.cir.0000028818.33488.7b
- Yellon DM, Hausenloy DJ. Myocardial reperfusion injury. *N Engl J Med*. 2007;357:1121–1135. doi: 10.1056/NEJMr071667
- Su H, Spinale FG, Dobrucki LW, Song J, Hua J, Sweterlitsch S, Dione DP, Cavaliere P, Chow C, Bourke BN, et al. Noninvasive targeted imaging of matrix metalloproteinase activation in a murine model of postinfarction remodeling. *Circulation*. 2005;112:3157–3167. doi: 10.1161/CIRCULATIONAHA.105.583021
- Liu YH, Sahul Z, Weyman CA, Dione DP, Dobrucki WL, Mekkaoui C, Brennan MP, Ryder WJ, Sinusas AJ. Accuracy and reproducibility of absolute quantification of myocardial focal tracer uptake from molecularly targeted SPECT/CT: a canine validation. *J Nucl Med*. 2011;52:453–460. doi: 10.2967/jnumed.110.082214
- Sahul ZH, Mukherjee R, Song J, McAteer J, Stroud RE, Dione DP, Staib L, Papademetris X, Dobrucki LW, Duncan JS, et al. Targeted imaging of the spatial and temporal variation of matrix metalloproteinase activity in a porcine model of postinfarct remodeling: relationship to myocardial dysfunction. *Circ Cardiovasc Imaging*. 2011;4:381–391. doi: 10.1161/CIRCIMAGING.110.961854
- Fedak PW, Altamentova SM, Weisel RD, Nili N, Ohno N, Verma S, Lee TY, Kiani C, Mickle DA, Strauss BH, et al. Matrix remodeling in experimental and human heart failure: a possible regulatory role for TIMP-3. *Am J Physiol Heart Circ Physiol*. 2003;284:H626–H634. doi: 10.1152/ajpheart.00684.2002

12. Kandalam V, Basu R, Abraham T, Wang X, Awad A, Wang W, Lopaschuk GD, Maeda N, Oudit GY, Kassiri Z. Early activation of matrix metalloproteinases underlies the exacerbated systolic and diastolic dysfunction in mice lacking TIMP3 following myocardial infarction. *Am J Physiol Heart Circ Physiol*. 2010;299:H1012–H1023. doi: 10.1152/ajpheart.00246.2010
13. Kruk M, Menon V, Kądziała J, Sadowski Z, Ruzylko W, Janas J, Roik M, Opolski G, Zmudka K, Czunko P, et al. Impact of percutaneous coronary intervention on biomarker levels in patients in the subacute phase following myocardial infarction: the Occluded Artery Trial (OAT) biomarker ancillary study. *BMC Cardiovasc Disord*. 2013;13:91. doi: 10.1186/1471-2261-13-91
14. Takawale A, Zhang P, Azad A, Wang W, Wang X, Murray AG, Kassiri Z. Myocardial overexpression of TIMP3 after myocardial infarction exerts beneficial effects by promoting angiogenesis and suppressing early proteolysis. *Am J Physiol Heart Circ Physiol*. 2017;313:H224–H236. doi: 10.1152/ajpheart.00108.2017
15. Yan AT, Yan RT, Spinale FG, Afzal R, Gunasinghe HR, Stroud RE, McKelvie RS, Liu PP. Relationships between plasma levels of matrix metalloproteinases and neurohormonal profile in patients with heart failure. *Eur J Heart Fail*. 2008;10:125–128. doi: 10.1016/j.ejheart.2007.12.002
16. Barlow SC, Doviak H, Jacobs J, Freeburg LA, Perreault PE, Zellars KN, Moreau K, Villacreses CF, Smith S, Khakoo AY, et al. Intracoronary delivery of recombinant TIMP-3 after myocardial infarction: effects on myocardial remodeling and function. *Am J Physiol Heart Circ Physiol*. 2017;313:H690–H699. doi: 10.1152/ajpheart.00114.2017
17. Eckhouse SR, Purcell BP, McGarvey JR, Lobb D, Logdon CB, Doviak H, O'Neill JW, Shuman JA, Novack CP, Zellars KN, et al. Local hydrogel release of recombinant TIMP-3 attenuates adverse left ventricular remodeling after experimental myocardial infarction. *Sci Transl Med*. 2014;6:223ra21. doi: 10.1126/scitranslmed.3007244
18. Purcell BP, Lobb D, Charati MB, Dorsey SM, Wade RJ, Zellars KN, Doviak H, Pettaway S, Logdon CB, Shuman JA, et al. Injectable and bioresponsive hydrogels for on-demand matrix metalloproteinase inhibition. *Nat Mater*. 2014;13:653–661. doi: 10.1038/nmat3922
19. Zavadzkas JA, Stroud RE, Bouges S, Mukherjee R, Jones JR, Patel RK, McDermott PJ, Spinale FG. Targeted overexpression of tissue inhibitor of matrix metalloproteinase-4 modifies post-myocardial infarction remodeling in mice. *Circ Res*. 2014;114:1435–1445. doi: 10.1161/CIRCRESAHA.114.303634
20. Xue CB, Voss ME, Nelson DJ, Duan JJ, Cherney RJ, Jacobson IC, He X, Roderick J, Chen L, Corbett RL, et al. Design, synthesis, and structure-activity relationships of macrocyclic hydroxamic acids that inhibit tumor necrosis factor alpha release *in vitro* and *in vivo*. *J Med Chem*. 2001;44:2636–2660. doi: 10.1021/jm010127e
21. Wells RG, Timmins R, Klein R, Lockwood J, Marvin B, deKemp RA, Wei L, Ruddy TD. Dynamic SPECT measurement of absolute myocardial blood flow in a porcine model. *J Nucl Med*. 2014;55:1685–1691. doi: 10.2967/jnumed.114.139782
22. Malka A, Meerkin D, Barac YD, Malits E, Bachner-Hinzenon N, Carasso S, Ertracht O, Angel I, Shofti R, Youdim M, et al. TVP1022: a novel cardioprotective drug attenuates left ventricular remodeling after ischemia/reperfusion in pigs. *J Cardiovasc Pharmacol*. 2015;66:214–222. doi: 10.1097/FJC.0000000000000267
23. Ndrepepa G, Mehilli J, Schwaiger M, Schühlen H, Nekolla S, Martinoff S, Schmitt C, Dirschinger J, Schömig A, Kastrati A. Prognostic value of myocardial salvage achieved by reperfusion therapy in patients with acute myocardial infarction. *J Nucl Med*. 2004;45:725–729.
24. Piper HM, Abdallah Y, Schäfer C. The first minutes of reperfusion: a window of opportunity for cardioprotection. *Cardiovasc Res*. 2004;61:365–371. doi: 10.1016/j.cardiores.2003.12.012
25. Umemura S, Nakamura S, Sugiura T, Tsuka Y, Shimojo M, Baden M, Iwasaka T. Preservation of myocardial viability within the risk area by intravenous nicorandil before primary coronary intervention in patients with acute myocardial infarction. *Nucl Med Commun*. 2008;29:956–962. doi: 10.1097/MNM.0b013e32830fdde7
26. Vilahur G, Casani L, Peña E, Juan-Babot O, Mendieta G, Crespo J, Badimon L. HMG-CoA reductase inhibition prior reperfusion improves reparative fibrosis post-myocardial infarction in a preclinical experimental model. *Int J Cardiol*. 2014;175:528–538. doi: 10.1016/j.ijcard.2014.06.040
27. Angeli FS, Shapiro M, Amabile N, Orcino G, Smith CS, Tacy T, Boyle AJ, Chatterjee K, Glantz SA, Grossman W, et al. Left ventricular remodeling after myocardial infarction: characterization of a swine model on beta-blocker therapy. *Comp Med*. 2009;59:272–279.
28. McCafferty K, Forbes S, Thiemermann C, Yaqoob MM. The challenge of translating ischemic conditioning from animal models to humans: the role of comorbidities. *Dis Model Mech*. 2014;7:1321–1333. doi: 10.1242/dmm.016741
29. Houser SR, Margulies KB, Murphy AM, Spinale FG, Francis GS, Prabhu SD, Rockman HA, Kass DA, Molkentin JD, Sussman MA, et al. American Heart Association Council on Basic Cardiovascular Sciences, Council on Clinical Cardiology, and Council on Functional Genomics and Translational Biology. Animal models of heart failure: a scientific statement from the American Heart Association. *Circ Res*. 2012;111:131–150. doi: 10.1161/RES.Ob013e3182582523
30. Shehata IE, Cheng CI, Sung PH, Ammar AS, El-Sherbiny IAE, Ghanem IGA. Predictors of myocardial functional recovery following successful reperfusion of acute ST elevation myocardial infarction. *Echocardiography*. 2018;35:1571–1578. doi: 10.1111/echo.14106
31. Mangion K, Carrick D, Carberry J, Mahrous A, McComb C, Oldroyd KG, Eteiba H, Lindsay M, McEntegart M, Hood S, et al. Circumferential strain predicts major adverse cardiovascular events following an acute ST-segment-elevation myocardial infarction. *Radiology*. 2019;290:329–337. doi: 10.1148/radiol.2018181253
32. Iyer RP, Jung M, Lindsey ML. MMP-9 signaling in the left ventricle following myocardial infarction. *Am J Physiol Heart Circ Physiol*. 2016;311:H190–H198. doi: 10.1152/ajpheart.00243.2016
33. Mani SK, Kern CB, Kimbrough D, Addy B, Kasiganesan H, Rivers WT, Patel RK, Chou JC, Spinale FG, Mukherjee R, et al. Inhibition of class I histone deacetylase activity represses matrix metalloproteinase-2 and -9 expression and preserves LV function postmyocardial infarction. *Am J Physiol Heart Circ Physiol*. 2015;308:H1391–H1401. doi: 10.1152/ajpheart.00390.2014
34. Siminelakis S, Kotsanti A, Kolaitis N, Niokou D, Vlachou I, Dimakopoulos G, Papadopolou C. Circulating matrix metalloproteinase 3 due to myocardial ischemia. *Heart Surg Forum*. 2009;12:E230–E234. doi: 10.1532/HSF98.20081152
35. Wagner DR, Delagardelle C, Ernens I, Rouy D, Vaillant M, Beissel J. Matrix metalloproteinase-9 is a marker of heart failure after acute myocardial infarction. *J Card Fail*. 2006;12:66–72. doi: 10.1016/j.cardfail.2005.08.002
36. Apple KA, Yarbrough WM, Mukherjee R, Deschamps AM, Escobar PG, Mingoa JT, Sample JA, Hendrick JW, Dowdy KB, McLean JE, et al. Selective targeting of matrix metalloproteinase inhibition in post-infarction myocardial remodeling. *J Cardiovasc Pharmacol*. 2006;47:228–235. doi: 10.1097/01.fjc.0000200989.23987.b8
37. Matsumura S, Iwanaga S, Mochizuki S, Okamoto H, Ogawa S, Okada Y. Targeted deletion or pharmacological inhibition of MMP-2 prevents cardiac rupture after myocardial infarction in mice. *J Clin Invest*. 2005;115:599–609. doi: 10.1172/JCI22304
38. Morishita T, Uzui H, Mitsuke Y, Amaya N, Kaseno K, Ishida K, Fukuoka Y, Ikeda H, Tama N, Yamazaki T, et al. Association between matrix metalloproteinase-9 and worsening heart failure events in patients with chronic heart failure. *ESC Heart Fail*. 2017;4:321–330. doi: 10.1002/ehf2.12137
39. Cerisano G, Buonamici P, Gori AM, Valenti R, Sciagrà R, Giusti B, Sereni A, Raspanti S, Colonna P, Gensini GF, et al. Matrix metalloproteinases and their tissue inhibitor after reperfused ST-elevation myocardial infarction treated with doxycycline. Insights from the TIPTOP trial. *Int J Cardiol*. 2015;197:147–153. doi: 10.1016/j.ijcard.2015.06.024
40. Cerisano G, Buonamici P, Valenti R, Moschi G, Taddeucci E, Giurlani L, Migliorini A, Vergara R, Parodi G, Sciagrà R, et al. Effects of a timely therapy with doxycycline on the left ventricular remodeling according to the pre-procedural TIMI flow grade in patients with ST-elevation acute myocardial infarction. *Basic Res Cardiol*. 2014;109:412. doi: 10.1007/s00395-014-0412-2
41. Hudson MP, Armstrong PW, Ruzylko W, Brum J, Cusmano L, Krzeski P, Lyon R, Quinones M, Theroux P, Sydłowski D, et al. Effects of selective matrix metalloproteinase inhibitor (PG-116800) to prevent ventricular remodeling after myocardial infarction: results of the PREMIER (Prevention of Myocardial Infarction Early Remodeling) trial. *J Am Coll Cardiol*. 2006;48:15–20. doi: 10.1016/j.jacc.2006.02.055